17th World Conference on Earthquake Engineering, 17WCEE
Sendai, Japan - September 13th to 18th 2020

Numerical Simulation of Novel Multiple-variable frequency pendulum isolator

Xu Liang [(1)], Lihui Wang [(2)], Qiang Han [(3)] , Shoushan Cheng [(4)] , Yan Mao [(5)]

[(1)] *Ph.D. Student, Key Laboratory of Urban Security and Disaster Engineering of Ministry of Education, Beijing University of Technology, Beijing 100124, China. E-mail: liangxu11@emails.bjut.edu.cn*
[(2)]*Lecturer, Key Laboratory of Urban Security and Disaster Engineering of Ministry of Education, Beijing University of Technology, Beijing 100124, China (corresponding author). E-mail: wlh2016@bjut.edu.cn*
[(3)]*Professor, Key Laboratory of Urban Security and Disaster Engineering of Ministry of Education, Beijing University of Technology, Beijing 100124, China. E-mail: qhan@bjut.edu.cn*
[(4)]*Research Fellow, Research Institute of Highway Ministry of Transport, Beijing, PR China, 100088. E-mail: ss.cheng@rioh.cn*
[(5)]*Associate Fellow, Research Institute of Highway Ministry of Transport, Beijing, PR China, 100088. E-mail: 17526927@qq.com*

Abstract

The variable frequency pendulum isolator is good seismic isolation device for bridge and building in high earthquake intensity regions. It is found that the VFPI improves the superstructure responses at the cost of larger isolator displacements, which may cause the girder falling of the bridge. To avoid the large isolator displacement and satisfy the requirements of the “two stage” seismic design of the bridge, a Multi-variable frequency pendulum isolator (MVFPI) with the descending and ascending equivalent stiffness is proposed in this paper. According to the design requirements, the piecewise function is selected as the section function of the sliding surface of the MVFPI, and the mechanical model of MVFPI is established. The piecewise function is composed of hyperbolic function and exponential function, which provide restoring force softening and hardening section respectively. The softening section of the restoring force is to control the structural acceleration response during the service ground motions and the hardening section is to limit the maximum displacement during the rare ground motions. The critical displacement between the softening section and the hardening section is determined by the designer to ensure that it does not exceed the critical displacement under the designed earthquake. And the amplitude displacement of the isolator is defined as the critical displacement multiplied by a factor larger than unity under the maximum considered earthquakes. The theoretical model of the MVFPI is established with ABAQUS program and the hysteresis property of the isolator is simulated by low-frequency cyclic loading. The Mises stress distribution of the isolator has also been studied. The analytical results show that: 1) The numerical simulation results are identical to the theoretical analysis, which proved the correctness of the theoretical model; 2) The hysteresis property of the MVFPI is favorable, compared with FPS, it has the effect of reducing the acceleration response of the structure when the movement less than the initial designed displacement and limiting the maximum displacement when it exceeds the initial designed displacement; 3) The stiffness of MVFPI is determined by the sliding surface function, which makes the period of the isolator being a variable value and avoiding the resonance phenomenon under the long period ground motions; 4) The residual displacement of MVFPI depends on both friction coefficient and the parameters of sliding surface function, which should be designed based on analysis to control the maximum acceleration and displacement.

Keywords: Multi-variable frequency pendulum isolator; low-frequency cyclic loading; numerical simulation.

1. Introduction

Seismic isolation strategy have significant effects on structures such as buildings, bridges and other potentially vulnerable structures under earthquake conditions. It can be known that seismic isolators are generally divided into rubber bearings (including the lead rubber bearing and high damping bearing) and the sliding friction bearing[1]. Compared with the rubber bearing, the friction sliding bearing has the characteristics of insensitivity to the frequency of earthquake and uncoupled mechanism of energy dissipating and restoring system[2][3]. Friction pendulum system (FPS) is a traditional sliding bearing invented by Zayas et al[4], and has been widely used in engineering practice to protect structures from the effects of earthquake disasters. It could control the fundamental vibration period and has the re-centring capacity by a simple concave spherical shape. However, severe practical difficulties have been found due to the fixed time-period[5]. One of the difficulties is that FPS needs to be designed for a specifc level (intensity) of ground excitation. A isolation system called variable frequency pendulum isolator (VFPI) has been proposed by Pranesh et al. The non-spherical sliding surface makes the amplitude dependent time-period and the softening mechanism of restoring force. It is found that the base shear and acceleration can be controlled by VFPI and several shaking table tests have proved that the responses of the structures with VFPI[6] .But, Sharma and Jangid[7] pointed out that VFPI improves the superstructure responses at the cost of larger isolator displacements. It may incur the unseating or uplift of supersturctures at severe ground motions.

A new material, shape memory alloy (SMA) has been used in many rubber bearings to limit the displacement and provide energy dissipation ability[8][9], but less investigation has not been found that it used in VFPI to control the displacement during strong ground motions. The new PTFE fabric has been test that it can be used in FPS bearing at the design compressive stress 100Mpa.

Herein, a isolation bearing named multiple-variable frequency pendulum isolator (MVFPI) has been proposed, basing on VFPI, the MVFPI has the softening and hardening mechanism of restoring force to reduce the acceleration at service earthquakes (design earthquake) and control the displacement at severe ground motion(maximum considered earthquakes) according the seismic design codes. Besides, the SMA-wires are used to limit the displacement when it exceeds the design value. A three-dimensional (3D) FE model of MVFPI was developed and and the stress cloud diagram of the MVFPI was analyzed to prepare for the subsequent test design.

2. MVFPI description

As can be seen from Fig.1, the MVFPI is composed with of upper and lower bearings plates, slider, PTFE fabric plates and SMA. According from the concept of the "two-stage" design method specified by China and Europe in seismic design, the bearing sliding surface is designed to reduce the variable curvature surface of the structure's seismic response at different seismic intensities as needed based on specifications [10][11]. In these specifications, the seismic inputs used for seismic design is determined based on the probability of exceeding a defined limit condition (such as "10% in 50 years" or "2% in 50 years") within a specific reference periods of “475” and “2475” years for the moderate earthquake and severe earthquake in Chinese code. Therefore, the geometric function of the variable curvature sliding surface is represented by a piecewise function. Fig.1c shows the composition of the geometric function of the sliding surface of the bearing. The piecewise function consists of a hyperbolic function and an exponential function. In the initial stage, the hyperbolic function reduces the rigidity of the isolator and reduces the acceleration response of the structure. After exceeding a certain displacement x_1, the exponential function increases the stiffness to achieve the purpose of limiting the structural displacement. When approaching the limit displacement, the SMA begins to be stretched to further provide a limit function to prevent the falling beam phenomenon caused by excessive displacement. The new PTFE fabric is also used in MVFPI, and its high compressive properties can provide higher load carrying capacity.

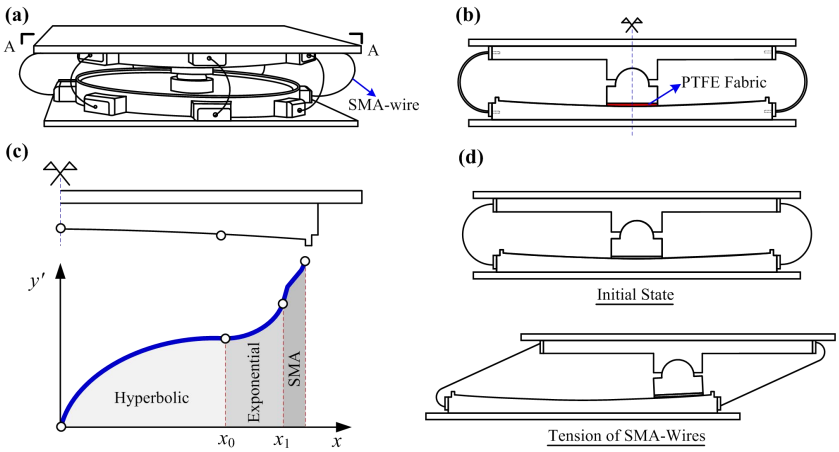

Fig.1 – The schematic diagram and A-A cross-section of the MVFPI

This subsection presents the force-displacement relationship of the MVFPI bearing. Before the derivation of the force-displacement relationship, the geometry equation of the sliding surface can be expressed as:

$$y=\begin{cases} b\sqrt{1+\dfrac{x^2}{(|x|+d)^2}}-b & x\le x_0 \\ y_0 e^{\frac{y_0'}{y_0}(x-x_0)} & x>x_0 \end{cases} \tag{1}$$

where, b and d are the parameters to depict the shape of the hyperbolic function; b is the value of y when x equal to zero and d is a constant. x_0 is the critical displacement between the hyperbolic function and the exponential function; y_0 is the value of the hyperbolic function at x_0; y'_0 is the first derivative of the hyperbolic function at x_0. It should be noted that the first-order derivative of the piecewise function is continuous at x_0.

During the SMA in tension, the restoring force F_r of the isolator is

$$F_r(x)=mg\frac{dy(x)}{dx}+nA\sigma\cos\theta=mgy'(x)+nA\sigma\cos\theta \tag{2}$$

where A is the area of a SMA wire, n is the number of SMA in the bearing;the constitutive model of the SMA can be described as follow:

$$\sigma=\begin{cases} k_1\varepsilon & \left(0\le\varepsilon\le\varepsilon_s^M, 0\le\varepsilon\le\varepsilon_f^A\right) \\ (k_1-k_2)\varepsilon_s^M+k_2\varepsilon & \left(\varepsilon_s^M\le\varepsilon\le\varepsilon_f^M\right) \\ (k_1-k_2)\left(\varepsilon_s^M-\varepsilon_f^M\right)+k_1\varepsilon & \left(\varepsilon_s^A\le\varepsilon\le\varepsilon_f^M\right) \\ (k_1-k_2)\varepsilon_f^A+k_2\varepsilon & \left(\varepsilon_f^A\le\varepsilon\le\varepsilon_s^A\right) \end{cases} \tag{3}$$

where, σ and ε are stress and strain in the SMA; k_1 and k_2 are elastic stiffness and post-activation stiffness; σ_s^a, σ_f^a, σ_s^m, σ_f^m and ε_s^a, ε_f^a, ε_s^m, ε_f^m are defined as the characteristic stresses and strains at austenite and martensite states.

Combining the above two components of the MVFPI, the general expression of the lateral force is expressed as follow:

$$F=\begin{Bmatrix} F_r+F_f & |x|\le x_1 \\ F_r+F_f+F_{SMA} & |x|>x_1 \end{Bmatrix}=\begin{Bmatrix} mgy'(x)+\mathrm{sgn}(\dot{x})umg & |x|\le x_1 \\ mgy'(x)+\mathrm{sgn}(\dot{x})umg+\mathrm{sgn}(x)nA\sigma\cos\theta & |x|>x_1 \end{Bmatrix} \tag{4}$$

3. Verification of FE Model

3.1 FE model

In order to verify the correctness of the hysteretic model of the MVFPI in the previous section, a 3D FE model was established using ABAQUS software. During the establishment, the solid element in ABAQUS was used to model the isolator. The surface parameters of the MVFPI are shown in the Table 1.

Table 1 – Parameters of MVFPI

Parameter	Parameter b /m	Parameter d /m	Initial period / s	Critical displacement /m	Friction coefficient	Maximum displacement /m
Value	0.161	0.30	1.5	0.1	0.05	0.16

To simulate the characteristics of the sliding, the bearing is controlled in the elastic force state, so the constitutive model of steel, PTFE fabric plate and SMA adopt the isotropic elastic model. The material properties are shown in the Table 2 and Table 3.

Table 2 – Material properties[12]

Bearing component	Material	Modulus (MPa)	Poisson ratio	Conductivity (mW/(mm K))	Specific heat (J/(kg K))
Bearing plates and sliders	Stainless steel	196000	0.3	46	5.0×10^5
PTFE fabric	PTFE	800	0.45	0.65	1.1×10^6

Table 3 – Material properties of SMA[13]

Bearing component	SMA-wire
Material	Sharp memory alloy
Modulus (MPa)	410000
Martensite'sPoisson ratio	0.33
Start of transformation(loading)	340
End of transformation(loading)	450
Start of transformation(unloading)	250
End of transformation(unloading)	100
Start of transformation in compression(loading)	459

To accurately simulate the sliding state of the MVFPI, the contact between the lower bearing plate and the sliding plate adopts surface-to-surface contact (Standard), in which the sliding surface of the lower bearing plate is the main surface, and the surface where the slide plate contacts the lower isolator plate is the slave surface. The sliding formula is finite slip. To ensure that the master surface is in precise contact with the slave surface, the slave node/surface adjustment is selected only to remove interference. In the contact action attribute, the tangential behavior friction formula uses a penalty function. The tangential friction force of the contact surface follows Coulomb's law, in which the friction coefficient μ is a constant. The correlation between the friction coefficient and speed and the magnitude of the friction force and the contact surface are both ignored. The friction force is proportional to the pressure, and it is assumed that the coefficient of dynamic friction is the same as the coefficient of static friction, which is taken as 0.05. The normal behavior uses hard contact, it means that the values of the contact pressure that can be transmitted between the contact surfaces unlimitedly; when the contact pressure becomes zero or negative, the two contact surfaces are separated and the contact constraints on the corresponding nodes are removed. It matches the actual working conditions of the friction pendulum bearings completely. The slider and the PTFE plate are bonded to simulate the paste state. The bottom surface of the slider is the main surface, and the surface where the PTFE plate and the slider in contact is the slave surface. The slider and the upper bearing plate also adopt the same parameters.

To simulate the sliding state of the isolator in the actual test and avoid side shift and torsion during the simulation, the boundary conditions of the isolator are set as follows: 1) The lower isolator plate of the isolator is set to a fixed end, and is set to be completely fixed, 2) The upper isolator plate is set as a loading end, which can be freely loaded but not allowed rotated. The vertical load is once loaded, and the horizontal load is cyclically

loaded with displacement control. During the load application, two analysis steps are used for calculation. The first step applies a vertical axial force of 500 kN. The second step applies a displacement load at the loading end. To save calculation time, 100% displacement amplitude is directly used.

The elements commonly used in finite element software are tetrahedral and hexahedral elements. When analyzing three-dimensional problems, hexahedral elements can be used to obtain the best calculation results at a low cost. Therefore, hexahedral elements are often used for three-dimensional problems. In this paper, the eight-noded brick-coupled thermal-mechanical elements (C3D8T) were used in the FE model. The refined finite element meshes were adopted for the PTFE fabric plate, as shown in Fig. 2(b). The slider is composed of a part of a sphere and a cylinder-like body. Before the mesh is divided, the geometric elements are first divided to facilitate the mesh division.

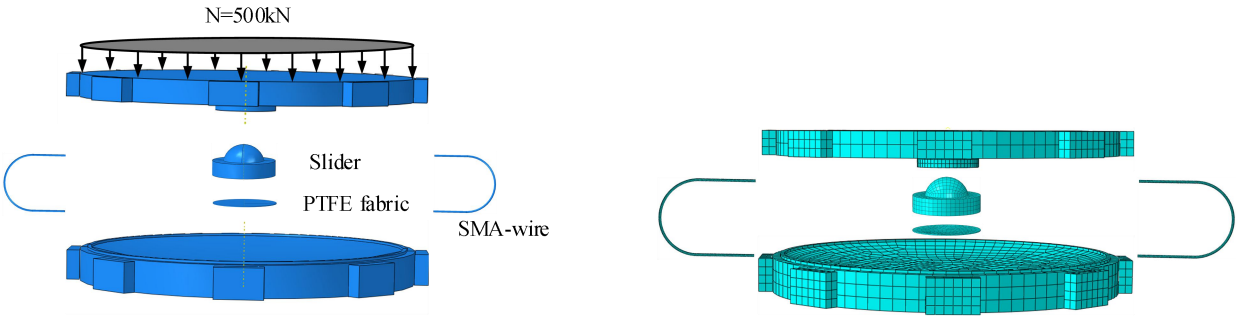

(a) Details of component parts (b) Finite element model

Fig.2 – FE model and meshes of the MVFPI

3.2 FE analyze result

The Fig.3 is the stress distribution (S, Mises) of the finite element analysis result. For the convenience of observation, the axisymmetric method will be used to model the isolator. The variable curvature friction pendulum isolator load in the finite element analysis is mainly divided into vertical load and horizontal load. Among them, the vertical load is to simulate the weight of the bridge structure in the actual application process, and the horizontal load is to simulate the force generated by the seismic vibration. According to the change law of the isolator stress, it can be known whether the strength design of the isolator meets the requirements and provides a reference for subsequent optimization of the isolator.

3.2.1 Vertical loading

The stress distribution of the bearing after vertical loading by the finite element simulation is shown in Fig3. It can be seen from Fig.3 that there is no sliding during the vertical loading stage, so the friction coefficient and horizontal slip have no significant effect on the stress distribution. During the loading phase, the stress distribution of the bearing is only related to the vertical load.

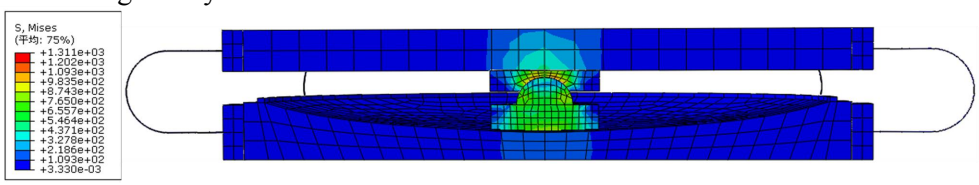

Fig. 3 – Axial compressive stress distribution of MVFPI

From Fig.4 to Fig.6 are the stress distribution of each component of the MVFPI at axial pressure. At the axial pressure, the compression area of the MVFPI is the PTFE fabric plate. Due to the variable curvature characteristics of the bearing, the stress is greater in the middle part of the lower sliding surface.

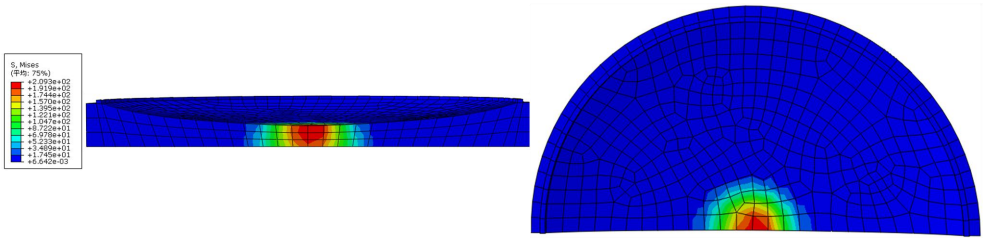

Fig. 4 – Axial compressive stress distribution of the lower bearing plate

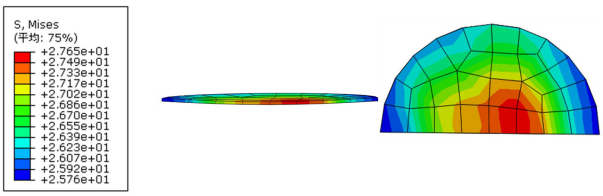

Fig.5 – Axial compression stress distribution cloud of PTFE plate

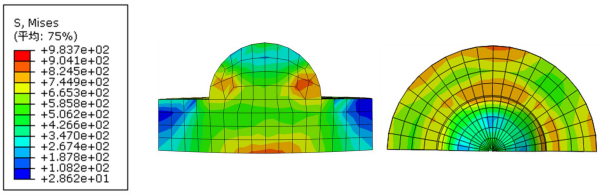

Fig.6 – Axial compressive stress distribution of the slider

3.2.3 Horizontal loading

Fig.7 shows the stress distribution of the bearing at a displacement of 60mm. After the horizontal displacement is loaded, the sliding occured between the upper bearing plate and the slider, and due to the change of the sliding surface and the influence of the friction coefficient, the stress of the bearing is unevenly distributed.

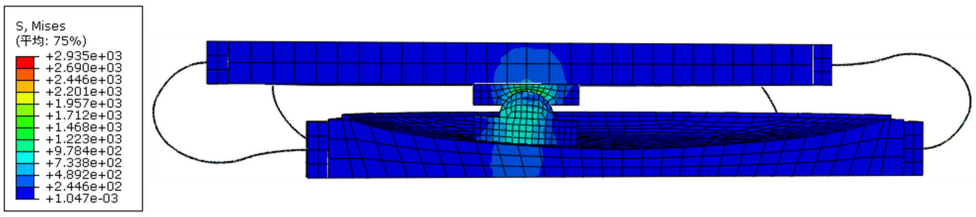

Fig.7 – Stress distribution at 60 mm of MVFPI

It can be seen from Fig.8 that at the sliding surface of the lower bearing plate, when the bearing is displaced by 60 mm, the curvature concentration of the sliding surface increases, and the bearing generates a stress concentration phenomenon under intermediate compression. As shown in Fig.9, this phenomenon is more obvious in PTFE slides, when the curvature radius of the sliding surface increases, the middle of the PTFE slide is subjected to the greatest force and the wear is more serious. Fig.10 are the stress distribution of the bearing slider at a bearing displacement of 60 mm.

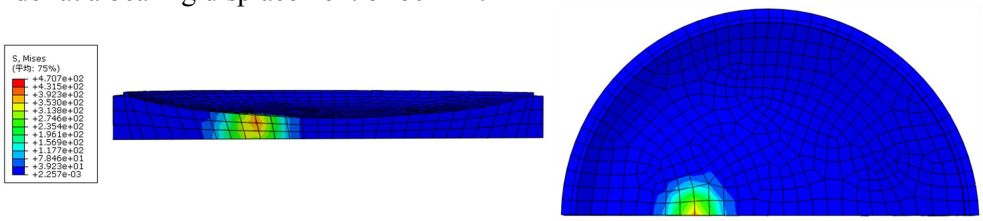

Fig. 8 – Stress distribution at 60 mm of the lower bearing plate

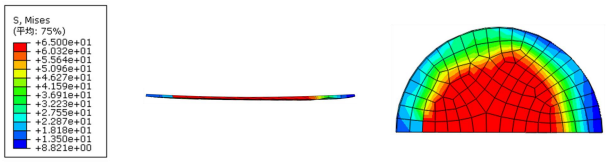

Fig. 9 – Stress distribution at 60mm of the PTFE plate

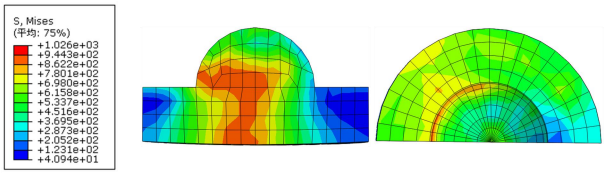

Fig.10 – Stress distribution at 60 mm of the slider

Fig.11 shows the stress cloud diagram of the isolator at a displacement of 150 mm. The SMA is in tension at this stage.

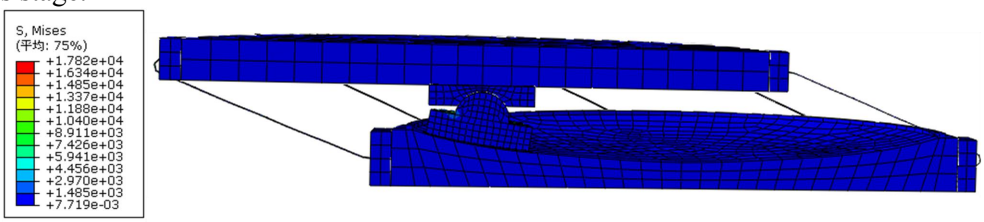

Fig.11 – Stress distribution at 150mm of MVFPI

It can be seen from Fig.12 that at the sliding surface of the lower bearing plate, when the bearing is displaced by 150 mm, the curvature radius of the sliding surface decreases, and the bearing generates a stress concentration phenomenon at both ends of the bearing. This phenomenon is more obvious in PTFE slides, as shown in Fig.13, which shows that when the radius of curvature of the sliding surface is reduced, the edges of the PTFE slides are stressed the most and serious wear may occur. Fig.14 are the stress distribution of the bearing slider at the maximum displacement of the bearing.

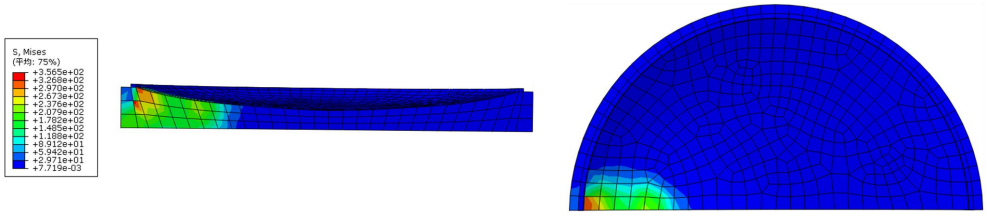

Fig. 12 – Stress distribution at 150 mm of the lower bearing plate

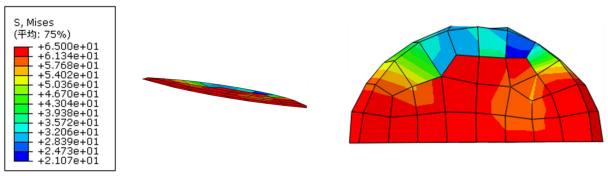

Fig.13 – Stress distribution at 150 mm of the PTFE plate

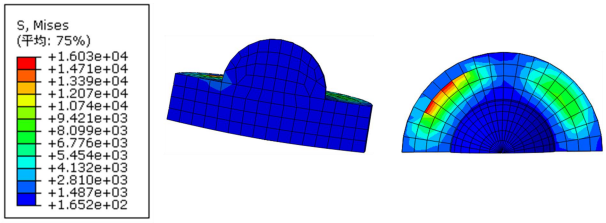

Fig.14 – Stress distribution at 150 mm of slider

3. Comparison of results

As shown in Fig.15, it can be seen that the finite element analysis results has a good agreement with the theoretical model, proving the feasibility of the MVFPI and the correctness of the theoretical results. It can be known from the stress distribution that in the simulation results, the cause of the bearing load unevenness may be due to different stress concentration phenomena of the bearing slider during the sliding process, but the overall trend is still in line with the theoretical results.

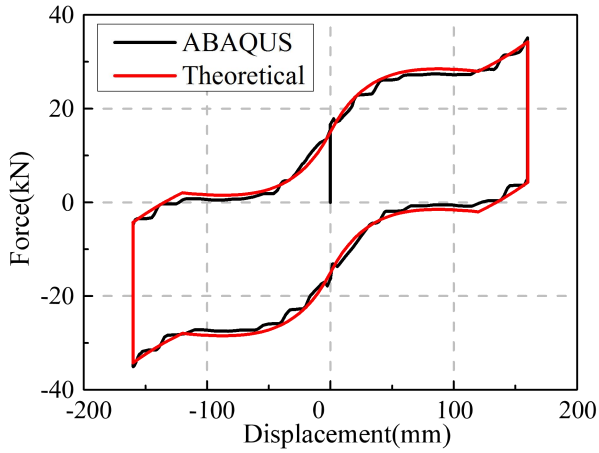

Fig. 15 – Comparison of FE model and theoretical results

There are clear difference between the softening stage and the hardening stage of the MVFPI bearing's restoring force. During the softening stage, the restoring force of the bearing is no longer increasing to reduce the acceleration response of the structure under a design earthquake, during the hardening stage, the restoring force of the bearing increases sharply to limit the structural displacement.

4. Results

In this study, a novel multiple-variable frequency pendulum isolator (MVFPI) with high-performance materials has been proposed and the underlying principles of operation were also introduced. The FE model was established and the finite element analysis was carried out. The stress distribution of the MVFPI was analyzed. The following conclusions can be drawn from the present study:

1) The numerical simulation results are identical to the theoretical analysis, which proved the correctness of the theoretical model;

2) The hysteresis property of the MVFPI is favorable, it has the effect of reducing the acceleration response of the structure when the movement less than the initial designed displacement and limiting the maximum displacement when it exceeds the initial designed displacement;

3) The stiffness of MVFPI is determined by the sliding surface function, which makes the period of the isolator being a variable value and avoiding the resonance phenomenon under the long period ground motions;

4) The stress distribution of the MVFPI shows that the stress concentration phenomenon in the stiffness softening stage is reflected in the center of the PTFE fabric, and in the stiffness strengthening section, the stress concentration phenomenon is reflected in edge of the plate. The anti-wear effect of the entire PTFE fabric needs to be taken into account.

5. Acknowledgements

This research is jointly funded by the National Key of Research and Development of China (2018YFC1504306), National Natural Science Foundation of China (NSFC) (Grants No. 51421005, 51838010) and Beijing Municipal Education Commission (IDHT20190504). These financial support are gratefully acknowledged. The results and conclusions presented in the paper are those of the authors and do not necessarily reflect the view of the sponsors.

6. References

[1] Tsopelas P, Constantinou M C, Okamoto S (1996): Experimental study of bridge seismic sliding isolation systems[J]. *Engineering Structures*, **18**(4): 301-310.

[2] Eröz, M , DesRoches, R. (2008): Bridge seismic response as a function of the Friction Pendulum System (FPS) modeling assumptions. *Engineering Structures*, **30**(11), 3204-3212.

[3] Almazán, J. L., & Llera, J. C. D. L. (2003): Physical model for dynamic analysis of structures with FPS isolators. *Earthquake engineering & structural dynamics*, **32**(8), 1157-1184.

[4] Zayas, V. A., Low, S. S., & Mahin, S. A. (1990):A simple pendulum technique for achieving seismic isolation. *Earthquake spectra*, **6**(2), 317-333.

[5] Pranesh, M. (2000). VFPI: An innovative device for aseismic design (*Doctoral dissertation, Ph. D. Thesis, Indian Institute of Technology, Bombay*).

[6] Cheng-Yen Wu (2004): Experiment and analysis of isolated structure with variable curvature sliding isolation [D]. *National Kaohsiung First University of Science and Technology*.

[7] Sharma A, Jangid R S (2012): Performance of variable curvature sliding isolators in base - isolated benchmark building [J]. *The Structural Design of Tall and Special Buildings*, **21**(5): 354-373.

[8] Dezfuli F H, Alam M S (2014): Performance-based assessment and design of FRP-based high damping rubber bearing incorporated with shape memory alloy wires [J]. *Engineering Structures*, **61**: 166-183.

[9] Shinozuka M, Chaudhuri S R, Mishra S K (2015): Shape-memory-alloy supplemented lead rubber bearing (SMA-LRB) for seismic isolation [J]. *Probabilistic Engineering Mechanics*, **41**: 34-45.

[10] JTJ/T B02-01-2008 Guidelines for Seismic Design of Highway Bridges [S].

[11] European Committee for Standardization (CEN) (2004): Design of structures for earthquake resistance, part 1: General rules, seismic actions and rules for buildings EN 1998-1 Eurocode 8 Brussels.

[12] Han Q, Wen J, Zhong Z (2018): Numerical Simulation of Frictional Heating Effects of Sliding Friction Bearings for Isolated Bridges [J]. *International Journal of Structural Stability and Dynamics*, **18**(08): 1840008.

[13] Wang B, Zhu S (2018): Superelastic SMA U-shaped dampers with self-centering functions [J]. *Smart materials and structures*, **27**(5): 055003.

